Dynamics of Antimatter-Atom Collisions

R. E. Olson and T. J. Gay

Laboratory for Atomic and Molecular Research, and Physics Department, University of Missouri-Rolla, Rolla, Missouri 65401

(Received 10 December 1987)

Classical-trajectory Monte Carlo calculations have been used to study ionizing collisions between charged particles ($p,\bar{p},e^+,e^-$) and He atoms at an incident velocity of 2.83 a.u. While differences in the total single-ionization cross sections for these projectiles are small, our calculations reveal large effects at all angles in the ionized electron spectra, and provide qualitative evidence for a Barkas effect in p and $\bar{p}$ collisions. Experimental data agree well with our fully classical calculations, including cross sections involving ejected electrons of long wavelength.

PACS numbers: 34.50.Fa, 34.80.Dp, 36.10.Dr

The process of electron emission resulting from ionization of atoms by fast, charged particles is ubiquitous. An understanding of the dynamics of electron ejection is a prerequisite for accurate descriptions of plasmas, ion-surface collisions, and the stopping of ions in solids. While modeling of a given physical process may require only the knowledge of total ionization cross sections, more often additional detailed information is needed, such as cross sections for electron ejection which are singly or even doubly differential in the energy and/or angle of ejection. Ionization dynamics can be probed directly by the use of projectiles of varying mass and charge sign. However, in the Bethe-Born theory, ionization cross sections depend on the square of the projectile's charge, and are independent of its mass. Nonetheless, evidence for charge-sign-dependent dynamical effects, such as the Barkas effect in stopping-power measurements, has existed for some time.[1,2] Several recent experiments have yielded intriguing data on total ionization cross sections for incident protons, electrons, and their antiparticles.[3-5] These effects have been investigated quantum mechanically[6,7] and classically.[8]

Measurements of the ejected electrons provide a particularly sensitive probe of ionizing collisions. Thus, variations in electron spectra caused by a change in the projectile's charge sign or mass provide a deeper insight into ionization dynamics than do comparable total cross-section measurements. There are now available relatively high fluxes of e^+ and low-energy $\bar{p}$ beams.[3-5] While matter-antimatter effects have recently been predicted in triply differential ionization cross sections for projectiles and electrons scattered to small angles,[9,10] these results are virtually untestable because of low counting rates and/or annihilation background from angle-defining slits. In this Letter, we predict large, global effects in singly differential cross sections for direct (as opposed to electron capture) ionization in the collisions

$$x + \mathrm{He} \rightarrow x + \mathrm{He}^+ + e^-, \qquad (1)$$

(where $x = p,\bar{p},e^+,e^-$) which should be experimentally observable.

Our classical-trajectory Monte Carlo (CTMC) calculations employ a complete classical description of the scattering process. They are based on the numerical solution of Hamilton's equations of motion for a three-dimensional, three-body system.[11] Unlike Born approximation techniques,[9] which in essence consider only the electron-target or electron-projectile interaction, the CTMC method essentially provides an infinite basis set for the collision system, and inherently includes the effects of two charge centers on the electron motion. The importance of such two-center effects has recently been recognized.[12-14]

The He target was described by the independent-electron model,[15] with an effective charge of 1.6875 and the experimental binding energy of 24.58 eV. It should be noted that the CTMC method directly includes the angular scattering of the projectile, the recoil of the target nucleus (which we have found to be important in the angular scattering of light projectiles), and the effects of electron capture (for positively charged projectiles).

We have performed these calculations for projectile velocities of 2.83 a.u. [p ($\bar{p}$) energies of 200 keV and e^+ (e^-) energies of 109 eV], because of the large amount of "benchmark" data available at or near this velocity for incident protons and electrons. Good agreement between our results and these data, especially for e^- projectiles, lends credibility to our predictions about the e^+ and $\bar{p}$ collisions, for which measurements appear to be feasible.

At this velocity, we note the similarity of total direct-single-ionization cross sections [reaction (1)]. Our calculated values for protons and positrons (in units of 10^{-17} cm^2) are 6.6 ± 0.2 and 5.2 ± 0.2, respectively, as compared with experimental results of 7.0 ± 0.7 for protons,[16] and 4.5 ± 0.4 for positrons.[4] The reason for this e^+-p difference is the partitioning of the free-electron flux between the direct-ionization and electron-capture-ionization channels. For positrons at this velocity, electron capture is enhanced by a factor of 4 over that for

protons as a result of the greater ability of the e^+ to match velocity vectors with the target electrons. The calculated values for e^- and $\bar{p}$ collisions are 4.5 ± 0.2 and 4.9 ± 0.2, respectively. The experimental value for electrons[17] is 3.9 ± 0.5. Thus, all the total cross sections are encompassed within a range of $5.5 \pm 28\%$.

In contrast, the singly differential cross sections in energy, shown in Fig. 1, reveal large differences in collision dynamics for the different projectiles. In comparing e^+ and e^- collisions, we note first a dramatic falloff of target e^- emission at the highest ejection energies with incident positrons. Examination of the trajectories for events in which a high-energy e^- is ejected shows that they involve "head-on" collisions between the projectile and the target e^-, in which momentum and energy are substantially exchanged. In the case of e^+ projectiles, however, such events cannot yield a high asymptotic electron energy for collisions close to the nucleus (where the probability of impact is greatest), because a significant fraction of the available collision energy (84 eV) will be dissipated in the e^+-He^+ Coulomb repulsion. For example, an ionized target e^- with a final energy of 65 eV must be struck by the e^+ when it is about

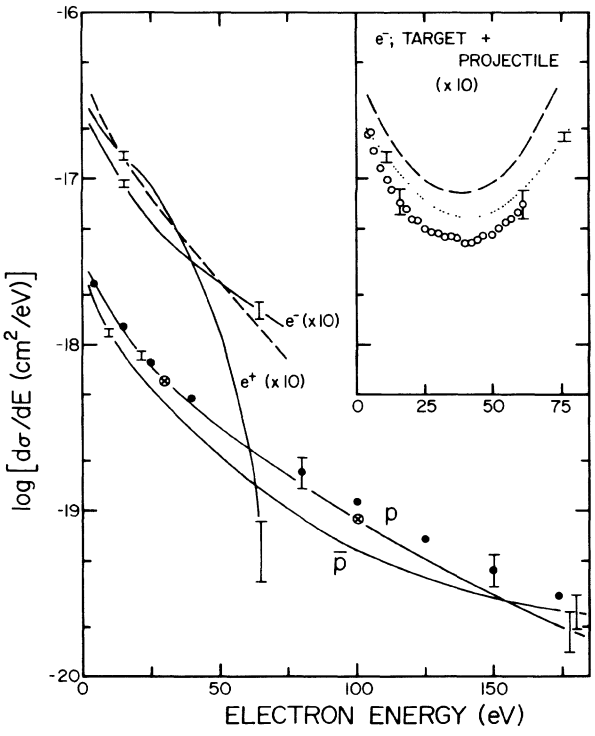

FIG. 1. He target electron ejection cross sections singly differential in ejected-electron energy. Solid and dotted lines represent the CTMC calculation; open and solid circles are the data of Refs. 18 and 19, respectively. Dashed lines are the Born approximation calculation of Manson (Ref. 20); crossed circles are Madison's Born approximation calculation (Ref. 21). Representative errors in the data and our CTMC calculation are indicated by vertical bars.

1.4 a.u. from the He^+; the probability of such a collision is low and is decreasing rapidly with distance from the nucleus. For completeness, we note that our calculations for total electron ejection cross sections (target + projectile) with e^- projectiles can be compared with experimental data taken at 100-eV incident energy[18] (see inset, Fig. 1). Both our results and the quantum-mechanical calculation of Manson[20] reproduce the shape of these cross sections quite well.

The electron spectra for protons and antiprotons are also shown in Fig. 1. For protons, our calculations are in excellent agreement with the quantum-mechanical results of Madison[21] and the data of Rudd, Toburen, and Stolterfoht.[19] Of particular interest is the fact that the proton cross sections are generally above those for antiprotons. This difference is seen in the more detailed doubly differential data to be due primarily to the additional contribution from "saddle-point" ionization[13] in the p case, in which electrons are left stranded in the Coulomb saddle-point region between the receding projectile and the ionized target. (Saddle-point ionization is also responsible for the enhancement of the e^+ cross sections over those for e^- projectiles at lower ejection energies.) We note also the lack of an analogous cross section falloff at high electron ejection energy with protons versus positrons, due to the proton's larger momentum.

The range of particles in matter depends on the integral

$$R = \int_0^{E_i} dE \left[\sum_j \int_0^E n\epsilon\, d\epsilon \left(\frac{d\sigma_j(E,\epsilon)}{d\epsilon} \right) \right]^{-1}, \qquad (2)$$

where ϵ is the energy lost by the projectile in the jth type of collision, $E(E_i)$ is the projectile's (initial) energy, and n is the target number density. To the extent that the integral in parentheses is dominated by $d\sigma/d\epsilon$ for ionizing collisions, the behavior of these cross sections for p and $\bar{p}$ collisions, seen in Fig. 1, would qualitatively explain the Barkas effect, or the fact that fast, negatively charged particles travel farther in solids than do positive ones. (Such a difference cannot be explained by energy loss resulting from charge transfer to the continuum; the total cross section associated with this mechanism is far too small.[13,22]) Further calculations by us indicate that $d\sigma/dE$ for protons lies above and is roughly parallel to that for antiprotons for $75 \lesssim E \leq 500$ keV. At energies $E \lesssim 75$ keV, electron capture maintains the dominance of the energy loss per collision for protons, while the $\bar{p}$ ionization cross section is decreasing rapidly. Above 500 keV, the cross sections are the same within our statistical uncertainties.

Easily observable differences between the various systems are predicted to occur in the singly differential ejected-electron spectra versus angle. In Fig. 2 we present these cross sections for incident protons and antiprotons. The proton results are in reasonable agreement with the experiments of Rudd, Toburen, and Stolter-

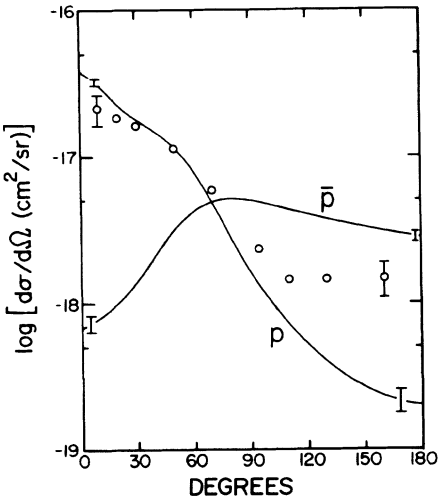

FIG. 2. He single-ionization cross sections singly differential in electron ejection angle. Solid lines: CTMC calculation. Data of Ref. 19.

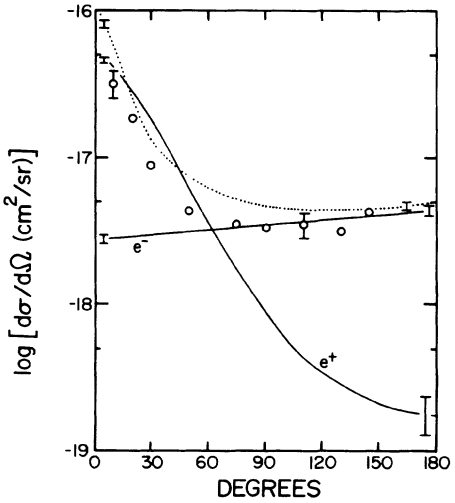

FIG. 3. He target electron ejection cross sections singly differential in ejection angle. Dotted line is the CTMC sum of target and projectile electrons, which can be compared to the data of Rudd and DuBois (Ref. 18).

foht,[19] except at large angles. New experimental evidence suggests that these large-angle data may, in fact, be high by an amount which would account for the discrepancy with our theory.[22] The $\bar{p}$ results diverge dramatically from those for protons; the angular differential cross sections differ by over an order of magnitude at both small and large scattering angles. The reason for these differences is easily understood classically; receding positive projectiles will tend to pull electrons out with them to small angles, whereas negative projectiles will repel ejected electrons to larger angles. Ejection at large angles also occurs preferentially with negative projectiles because of the antibinding or "Coulomb explosion" mechanism,[8,23] in which the projectile screens the target's nuclear field.

Behavior qualitatively similar to that seen with protons and antiprotons is predicted for e^+ and e^- projectiles (Fig. 3). At small angles the e^- projectile yields a much larger cross section than that predicted for antiprotons (Fig. 2). A low-mass projectile such as an e^- can undergo large deflections and still eject target electrons to small angles. In contrast, antiprotons are scattered to angles $\lesssim 0.1°$, and are thus much more effective at inhibiting emission at small angles. Comparing our calculations directly with experimental results by summing the cross secitons resulting from both the target atom and incident beam, we find good agreement with available data.[18]

These large differences between matter and antimatter spectra should be observable experimentally. With presently available e^+ fluxes of $10^7\ s^{-1}$ at Brookhaven National Laboratory,[24] the cross sections of Fig. 3 at, e.g., 150° yield nominal counting rates of 3 Hz for positrons versus roughly 100 Hz for electrons. Experiments measuring cross sections of this type can be expected to have relatively low annihilation backgrounds by virtue of the fact that no energy analysis need be made on the scattered electrons. Low-energy $\bar{p}$ beams at LEAR have intensities of $\sim 10^5\ s^{-1}$, with rather broad energy distributions.[3] However, current time-of-flight techniques being implemented will make measurements of $d\sigma/d\theta$ below 500 keV feasible with present beam-time allotments.[25] We find similar p-$\bar{p}$ differences at large and small angles for projectile energies to 500 keV, although the total ionization cross sections are dropping rapidly.

While we are primarily concerned with the different ionization dynamics which results from the use of projectiles with varying mass and charge sign, a second interesting result of this work is the demonstration that fully classical methods can describe the scattering of electrons at intermediate energies ($E \approx 100$ eV) where their de Broglie wavelengths are large. Indeed, it appears that the CTMC method is superior to available quantum methods at these energies because of the effectively infinite basis set used to describe the continuum. To test more stringently the range of validity of the CTMC method, we have calculated doubly differential cross sections for the systems under study. For all projectiles, study of electrons ejected at 13.6 and 27.2 eV (and at 109 eV for p and $\bar{p}$ projectiles) reveals even more marked differences at all angles than do the singly differential cross sections. Good agreement with available experimental data was realized in all of the above cases. As one example, we show in Fig. 4 our results for e^+ and e^- collisions at an ejected electron energy of 13.6 eV. de Broglie wavelengths for the incident projectile and ejected electron are 2.2 and 6.3 a.u., respectively. Focusing on the values for e^- projectiles, we find that most of the 13.6-eV electrons are ejected from the target except at small angles, where the projectile can strike the target

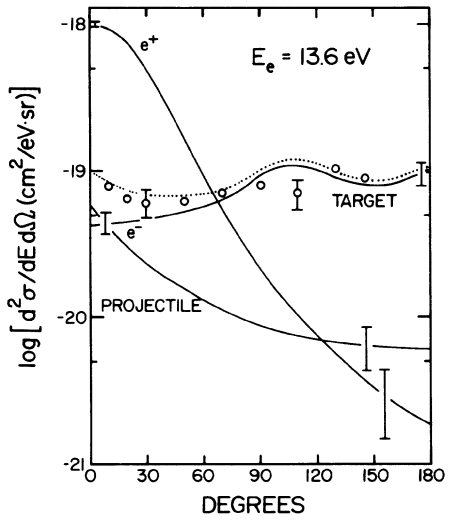

FIG. 4. Electron ejection cross sections doubly differential in ejection angle and energy. Data of Rudd and DuBois (Ref. 18); dotted line represents sum of target and projectile contributions.

electron head on, thus creating a fast target electron and a slow (e.g., 13.6 eV) projectile electron. Summing both cross sections we obtain the dotted curve which is in very good agreement with the absolute cross sections of Rudd and DeBois.[18]

In conclusion, we predict large global effects in the ejected-electron spectra for ionizing collisions when the charge sign and mass of the projectile are varied. Experiments that can observe this behavior appear to be tractable at this time. Such studies will yield important information on ionization dynamics. Furthermore, it appears that classical methods have a wider range of applicability than had been previously expected, and can provide quantitative estimates of detailed differential cross sections, even for light projectiles such as electrons.

This work was supported by the Office of Fusion Energy–Department of Energy and the National Science Foundation (Grant No. PHY-8602066).

[1]G. Basbas, Nucl. Instrum. Methods Phys. Res., Sect. B **4**, 227 (1984), and references therein.

[2]See, e.g., M. Inokuti, Y. Itikawa, and J. E. Turner, Rev. Mod. Phys. **50**, 23 (1978).

[3]L. H. Anderson, P. Hvelplund, H. Knudsen, S. P. Moller, and A. H. Sorensen, Phys. Rev. A **36**, 3612 (1987).

[4]D. Fromme, G. Kruse, W. Raith, and G. Sinapius, Phys. Rev. Lett. **57**, 3031 (1986).

[5]L. M. Diana, P. G. Coleman, D. L. Brooks, P. K. Pendleton, and D. M. Norman, Phys. Rev. A **34**, 2731 (1986).

[6]J. F. Reading and A. L. Ford, Phys. Rev. Lett. **58**, 543 (1987).

[7]M. H. Martir, A. L. Ford, J. F. Reading, and R. L. Becker, J. Phys. B **15**, 1729 (1982).

[8]R. E. Olson, Phys. Rev. A **36**, 1519 (1987).

[9]M. Brauner and J. S. Briggs, J. Phys. B **19**, L325 (1986).

[10]See, e.g., P. Mandal, K. Roy, and N. C. Sil, Phys. Rev. A **33**, 756 (1986).

[11]R. E. Olson and A. Salop, Phys. Rev. A **16**, 531 (1977).

[12]W. Meckbach, P. J. Focke, A. R. Goni, S. Suarez, J. Macek, and M. G. Menendez, Phys. Rev. Lett. **57**, 1587 (1986).

[13]R. E. Olson, T. J. Gay, H. G. Berry, E. B. Hale, and V. D. Irby, Phys. Rev. Lett. **59**, 36 (1987).

[14]N. Stolterfoht, D. Schneider, J. Tanis, H. Altevogt, A. Salin, P. D. Fainstein, R. Rivarola, J. P. Grandin, J. N. Scheurer, S. Andriamonje, D. Bertault, and J. F. Chemin, Europhys. Lett. **4**, 899 (1987).

[15]J. M. Hansteen and O. P. Mosebekk, Phys. Rev. Lett. **29**, 1361 (1972).

[16]M. E. Rudd, Y.-K. Kim, D. H. Madison, and J. W. Gallagher, Rev. Mod. Phys. **57**, 965 (1985).

[17]C. F. Barnett, J. A. Ray, E. Ricci, M. I. Wilker, E. W. McDaniel, E. W. Thomas, and H. B. Gilbody, Oak Ridge National Laboratory Report No. 5207, 1977 (unpublished).

[18]M. E. Rudd and R. D. DuBois, Phys. Rev. A **16**, 26 (1977); R. D. DuBois, private communication. See also, e.g., R. Müller-Fiedler, K. Jung, and H. Ehrhardt, J. Phys. B **19**, 1211 (1986), and references therein.

[19]M. E. Rudd, L. H. Toburen, and N. Stolterfoht, At. Data Nucl. Data Tables **18**, 413 (1976). The differential cross sections from this paper have been multiplied by 0.777 to yield the revised total cross section of Ref. 11.

[20]S. T. Manson, as cited by Rudd and DuBois, Ref. 18.

[21]D. H. Madison, Phys. Rev. A **8**, 2449 (1973).

[22]D. K. Gibson and I. D. Reid, J. Phys. B **19**, 3265 (1986).

[23]G. Mehler, B. Müller, W. Greiner, and G. Soff, Phys. Rev. A **36**, 1454 (1987).

[24]M. Weber, K. G. Lin, L. O. Roellig, A. P. Mills, Jr., and A. R. Moodenbaugh, in *Atomic Physics with Positrons,* edited by J. W. Humberston (Plenum, New York, 1988).

[25]E. Uggerhøj, private communication.